2010 IEEE International Conference on Robotics and Automation
Anchorage Convention District
May 3-8, 2010, Anchorage, Alaska, USA

Distributed Motion Control of Multiple Passive Object Handling Robots Considering Feasible Region of Brake Control

Yasuhisa Hirata, Yosuke Ojima and Kazuhiro Kosuge

Abstract— **This paper proposes a distributed motion control algorithm of multiple passive mobile robots for handling an object in cooperation with a human. The driving force of the passive mobile robot is an actual force applied by the human and the servo brakes attached to the wheels control its motion. Different from the active-type robot with servo motors, the passive robot has the control limitation based on the brake constraint. In this paper, we consider a feasible region for the brake control of the robot and propose a distributed motion control algorithm of the multiple passive mobile robots for handling a large object along the desired path, in which each robot compensates the control input required by other robots which do not generate it because of the brake constraint. We apply the proposed algorithm to two passive mobile robots called PRP experimentally and they realize an object handling along the desired path accurately.**

I. INTRODUCTION

We could apply robots to many fields such as home, office, medical etc. for supporting the humans. Especially, the physical supports for reducing the burdens of the humans or assisting the disability of the handicapped person including the elderly are essential functions of the robots. We have to consider the safety of human for realizing the physical interaction between the robot and the human.

From the viewpoint of the safety, Goswami et. al. proposed the concept of passive robotics [1], in which a system moves passively based on external force/moment without using servo motors, and have dealt with the passive wrist, whose components are springs, hydraulic cylinders, dampers, and so on. Peshkin et al. have also developed an object handling system called Cobot [2] based on passive robotics, which consists of the caster and the servo motor for steering its caster. These passive systems are intrinsically safe compared to the robot systems with active actuators such as servo motors, because they do not move automatically even if we cannot control them appropriately.

We have also developed passive intelligent walker called RT Walker to support the walking of the handicapped people including the elderly [3]. We pay attention to the brakes attached to the wheels for controlling the motion of the RT Walker. Break function is the important and essential for the mobile systems to limit the velocity of them. The RT Walker controls servo brakes attached to the wheels appropriately without using any servo motors and realizes several functions such as navigation function and gravity compensation function.

This research was partially supported by the Ministry of Education, Science, Sports and Culture, Grant-in-Aid for Young Scientists (A), 19686028, 2009

Y. Hirata, Y. Ojima and K. Kosuge are with Department of Bioengineering and Robotics, Tohoku University, 6-6-01, Aoba, Aramaki, Aoba-ku, Sendai 980-8579, Japan {hirata, ojima, kosuge}@irs.mech.tohoku.ac.jp

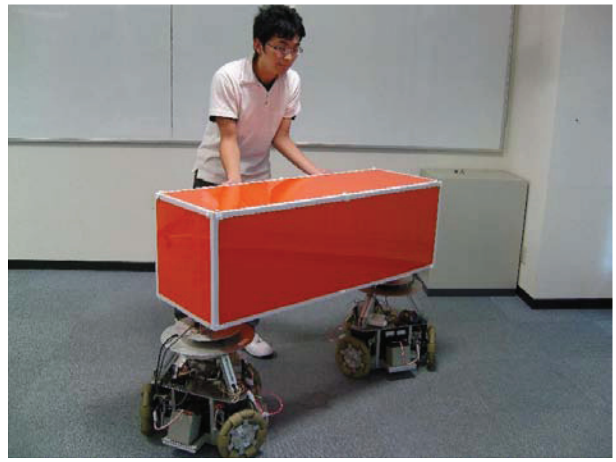

Fig. 1. Handling an Object by Multiple Passive Mobile Robots

We have also extended the brake control technologies of the RT Walker to the control of the omnidirectional-type object handling robot called PRP (Passive Robot Porter) [4]. In [4], we analyzed the conditions of the servo brake control and derived the feasible region of the brake control theoretically for realizing the desired motion of the PRP such as collision avoidance motion.

In the conventional researches on the passive mobile robot for handling an objec, researchers have considered the controls of the single mobile robot such as Cobot and PRP which are the natural extension from the researches on active-type robot with servo motors. On the other hand, in this paper, we consider the multiple mobile robots coordination for handling a large or a long object in cooperation with a human as shown in Fig. 1. Similar to the coordination by multiple robots with servo motors proposed by many researchers, e.g. [5], [6], [7], the coordination using multiple passive robots has advantages to improve the maneuverability for handling a large or a long object.

Different from the control method of robots with servo motors, the motion control of passive robots is challenging, because the passive robots cannot generate the motion we expected arbitrarily and the brake system only prevents the motion of the robot generated by the external force applied to it. But, when we consider the collaboration of the multiple passive mobile robots, we could solve the problem of the servo brake constraint explained above. Even if a passive

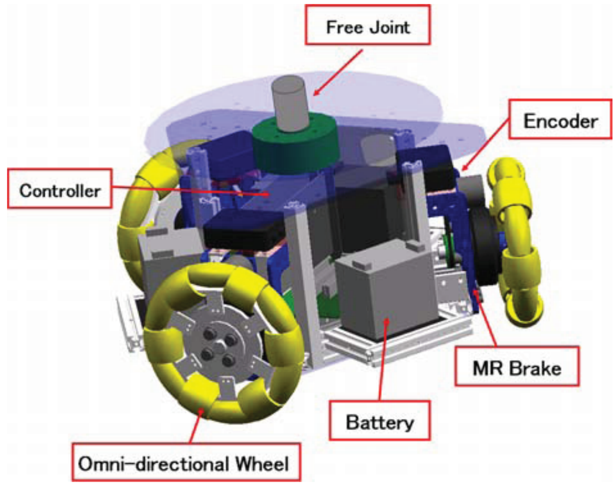

Fig. 2. Components of Omni-directional Passive Mobile Robot Called PRP

robot cannot generate the required motion because of the brake constraint, other passive robots might be able to assist the robot that cannot generate the required motion and the multiple passive robots could realize the tasks as the results. The collaboration of multiple passive robots has advantages that the robots can realize not only the handling of a large object but also the compensation of the force required for the desired handling tasks among robots.

For realizing the collaboration of multiple passive robots, firstly, we consider a feasible brake force region of the passive mobile robots with brakes, and based on the this brake constraint, we propose a distributed motion control algorithm of the multiple passive mobile robots, in which each robot estimates the feasibility of the required motion of other robots and compensates the insufficient motion of other robots. Finally, we apply the proposed algorithm to two omnidirectional passive robots experimentally and they handle a large object along the desired path in cooperation with a human for illustrating the validity of the proposed algorithm.

II. Control of Passive Mobile Robot

A. Hardware of PRP (Passive Robot Porter)

We have developed the passive robot porter called PRP based on the concept of the passive robotics [4] as shown in Fig. 2. The PRP consists of three omnidirectional wheels with servo brakes. The omnidirectional wheel consists of several small free rollers so that the wheel can move in all directions. Each omnidirectional wheel is directly connected to a servo brake. Three encoders are also installed on these wheels for odometry. We used MR Brake (Magneto-Rheological fluid Brake: Lord Corp., MRB-2107-3, Maximum on-state Torque: 5.6[Nm]) as the servo brake. It provides brake torque with high response and good linearity according to the input current.

In addition, the PRP carries an object through a free joint and has an encoder in it for measuring the relative angle between the object and the robot. By using the free joint, the PRP controls only the position of the object without considering its orientation. This means that the brake torques of wheels are only used for controlling the position of the object and the required force of the human operator for handling the object could be reduced [8]. The reduction of the required force of the human operator is necessary for passive robots.

B. Control Condition of Servo Brake

The PRP moves based on only the external force applied to it, because it does not have any active actuators such as servo motors. It is obvious that the characteristics of the brake system of wheel are complicated compared to a motor-wheel system. The characteristic of brake system depends on the wheel rotational direction. The sign of output torque of the wheel is decided by the direction of the wheel rotation and magnitude of the torque is proportional to the input current of the brake. We have the following condition between the angular velocity of the wheel and the braking torque of a brake-wheel system.

$$\tau_w \dot{\phi}_w \leq 0 \tag{1}$$

where τ_w is the brake torque of the wheel generated by the servo brake and $\dot{\phi}_w$ is the angular velocity of the wheel with servo brakes. This condition is the servo brake control constraint of the system and indicates that the braking torque and the wheel angular velocity are in different direction. Therefore we need to consider the feasible brake torque τ_w based on the motion of the robot [4].

C. Feasible Braking Force Based on Servo Brake Constraint

We can express the relation between braking torque $\boldsymbol{\tau}_w = [\tau_{w_1}, \tau_{w_2}, \tau_{w_3}]^T$ generated by wheels and resultant braking force ${}^{ob}\boldsymbol{F}_w = \left[{}^{ob}f_{wx}, {}^{ob}f_{wy}, 0\right]^T$ applied to the object by a PRP as follows:

$${}^{ob}\boldsymbol{F}_w = (\boldsymbol{J}^T)^{-1}\, \boldsymbol{\tau}_w \tag{2}$$

where $\boldsymbol{J}$ is Jacobian determined by the arrangement of the wheels. Subscript ob expresses the variables with respect to the object coordinate system ${}^{ob}\Sigma$ attached to on the free joint which is the center of the robot and it rotates with the free joint. Note that the robot carries the object through the free joint so that it cannot apply the moment to the object. This means that we do not consider the moment for controlling the orientation of the robot.

Since the brake torque of each wheel is depended on the direction of the wheel rotation as expressed in eq.(1), we have to consider that the servo brakes apply several kinds of torques to the robot according to the motion types of the PRP as shown in Tab. I. We discuss the feasible braking torque in each motion type. U_j denotes the set of feasible braking torque when the PRP is in j-th motion type $(j = 1, 2, \cdots, 8)$, and $A(U_j)$ denotes the resultant feasible force set of the robot from the feasible braking torque set U_j

$$U_j = \left\{ \tau_{w_1}\mathbf{e}_1 + \tau_{w_2}\mathbf{e}_2 + \tau_{w_3}\mathbf{e}_3 \mid \tau_{w_i}\dot{\phi}_{w_i} \leq 0\ ,\ |\tau_{w_i}| \leq \tau_{max} \right\} \tag{3}$$

TABLE I
MOTION TYPES BASED ON BRAKE CONDITIONS OF PRP

	Sign of Angular Wheel Velocity							
Wheel 1	+	+	+	+	-	-	-	-
Wheel 2	+	+	-	-	+	+	-	-
Wheel 3	+	-	+	-	+	-	+	-
Motion type No.	1	2	3	4	5	6	7	8

where,

$$\left[\begin{array}{ccc}\mathbf{e}_1 & \mathbf{e}_2 & \mathbf{e}_3\end{array}\right] = diag(1,1,1) \tag{4}$$

$$A(U_j) = \left\{\tau_{w1}\mathbf{v}_1 + \tau_{w2}\mathbf{v}_2 + \tau_{w3}\mathbf{v}_3 \;\middle|\; \tau_{w_i} \in U_j\right\} \tag{5}$$

where,

$$\left[\begin{array}{ccc}\mathbf{v}_1 & \mathbf{v}_2 & \mathbf{v}_3\end{array}\right] = (\boldsymbol{J}^T)^{-1}\left[\begin{array}{ccc}\mathbf{e}_1 & \mathbf{e}_2 & \mathbf{e}_3\end{array}\right] \tag{6}$$

Fig. 3(a) and (b) show the sets of U_j and $A(U_j)$, respectively, when the PRP is in Case 2. U_j is a quadrant of the braking torque configuration space with six plane constraints. The three constraint planes connected to the origin of the coordinates are the braking torque constraints. The other three constraint planes are from maximum torque limitation of each servo brake.

The each axis of the coordinate system shown in Fig. 3(b) expresses the possible force generated by the PRP. Based on the motion which belongs to one motion type in Case $1 \cdots 8$, the resultant feasible force ${}^{ob}\boldsymbol{F}_w$ and its corresponding braking torque $\boldsymbol{\tau}_w$ could be determined uniquely.

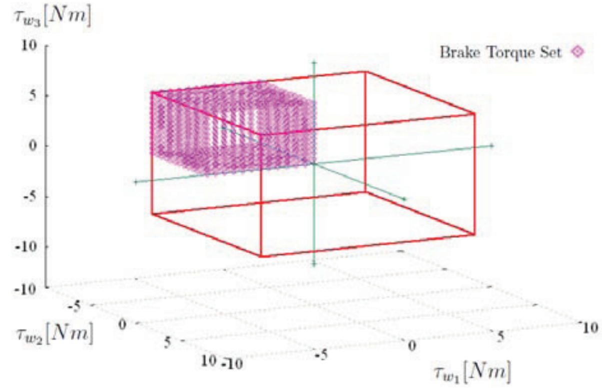

(a) Wheel Braking Torque Set U_2

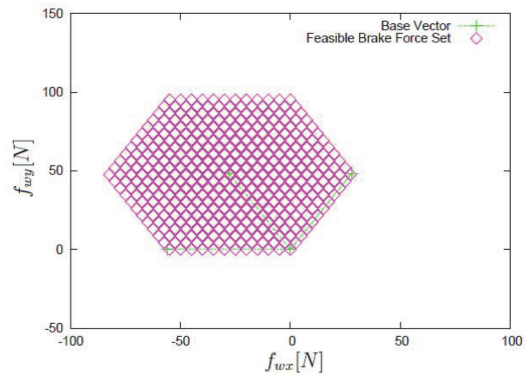

(b) Feasible Force Set $A(U_2)$

Fig. 3. Derivation of Feasible Force for Control of PRP

D. Motion Control of PRP Based on Feasible Braking Force

When the system considered here is that a human operator is always pushing an object supporting by k-th PRP, the dynamics of k-th robot including object can be represented as the following equation with respect to the translational motion.

$${}^{ob}\boldsymbol{M}_k {}^{ob}\ddot{\boldsymbol{q}}_{r_k} + {}^{ob}\boldsymbol{D}_k {}^{ob}\dot{\boldsymbol{q}}_{r_k} = {}^{ob}\boldsymbol{F}_{h_k} + {}^{ob}\boldsymbol{F}_{w_k} \tag{7}$$

where ${}^{ob}\dot{\boldsymbol{q}}_{r_k} \in \boldsymbol{R}^{2\times1}$, ${}^{ob}\ddot{\boldsymbol{q}}_{r_k} \in \boldsymbol{R}^{2\times1}$ are the velocity and the acceleration of the PRP. ${}^{ob}\boldsymbol{M}_k \in \boldsymbol{R}^{2\times2}$ is the inertial matrix of the handling object including the inertia of the PRP, ${}^{ob}\boldsymbol{D}_k \in \boldsymbol{R}^{2\times2}$ is the damping coefficient matrix of the robot and ${}^{ob}\boldsymbol{F}_{w_k} \in \boldsymbol{R}^{2\times1}$ is the feasible braking force generated by the servo brake of the PRP. ${}^{ob}\boldsymbol{F}_{h_k} \in \boldsymbol{R}^{2\times1}$ is the driving force of the robot applied by a human.

For realizing the desired motion of the robot in real time, we define a virtual force ${}^{ob}\boldsymbol{F}_{v_k} \in \boldsymbol{R}^{2\times1}$. It is determined by the control law of the robot for realizing the several functions such as path tracking, obstacle collision avoidance, impedance control, etc. If the virtual force ${}^{ob}\boldsymbol{F}_{v_k}$ is within the feasible force set in the current motion of the PRP which is determined by the sign of the angular velocities of the wheels explained in the previous section, we can command the brake torques of the wheels directly as ${}^{ob}\boldsymbol{F}_{w_k} = {}^{ob}\boldsymbol{F}_{v_k}$. On the other hand, of course, many cases exist that the virtual force ${}^{ob}\boldsymbol{F}_{v_k}$ is located out of the feasible set of the force, and cannot be generated by servo brakes. One typical example is that a passive robot cannot generate force for accelerating the motion of the object by itself.

To solve this problem, we consider a control algorithm of the passive robot. The force applied by the human ${}^{ob}\boldsymbol{F}_{h_k}$ could be divided into two elements. One is the driving force ${}^{ob}\boldsymbol{F}_{t_k}$ utilized for the transportation of the object along the pushing direction of the human, and the other is the assistive force ${}^{ob}\boldsymbol{F}_{a_k}$ for realizing the several functions such as path tracking. This relationship is illustrated by the following equation.

$${}^{ob}\boldsymbol{F}_{h_k} = {}^{ob}\boldsymbol{F}_{t_k} + {}^{ob}\boldsymbol{F}_{a_k} \tag{8}$$

We consider an apparent dynamics of the PRP expressed as follows:

$${}^{ob}\boldsymbol{M}_k {}^{ob}\ddot{\boldsymbol{q}}_{r_k} + {}^{ob}\boldsymbol{D}_k {}^{ob}\dot{\boldsymbol{q}}_{r_k} = {}^{ob}\boldsymbol{F}_{t_k} + {}^{ob}\boldsymbol{F}_{v_k} \tag{9}$$

This equation means that the PRP moves based on the driving force ${}^{ob}\boldsymbol{F}_{t_k}$ and the virtual force ${}^{ob}\boldsymbol{F}_{v_k}$ for realizing several functions such as path tracking, obstacle collision avoidance, and so on. From eq.(7) - eq.(9), we derive the following equation with respect to the braking force and moment ${}^{ob}\boldsymbol{F}_{w_k}$.

$${}^{ob}\boldsymbol{F}_{w_k} = {}^{ob}\boldsymbol{F}_{v_k} - {}^{ob}\boldsymbol{F}_{a_k} \tag{10}$$

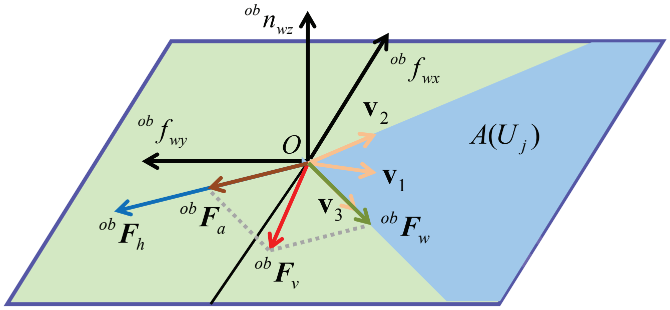

Fig. 4. Control of PRP Based on Feasible Braking Force

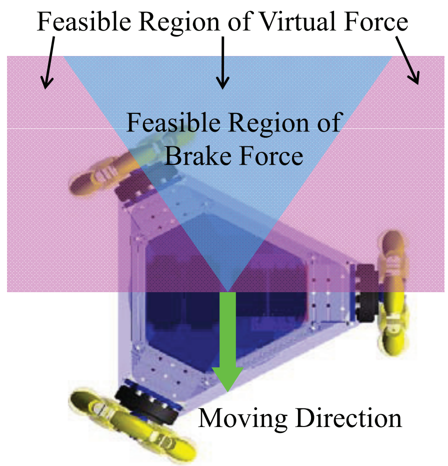

Fig. 5. Feasible Region of Virtual Force

Eq.(10) means that the virtual force $^{ob}\boldsymbol{F}_{v_k}$ is generated by the composition of the feasible brake force $^{ob}\boldsymbol{F}_{w_k}$ and the assistive force $^{ob}\boldsymbol{F}_{a_k}$ which is a part of the force applied by the human as shown in Fig. 4. When we specify the feasible brake force $^{ob}\boldsymbol{F}_{w_k}$ based on the above equation, the apparent dynamics of the PRP expressed by eq.(9) is realized without identifying the real inertial and damping parameters of object and robots.

That is, even if $^{ob}\boldsymbol{F}_{v_k}$ is out of the feasible brake force set $A(U_j)$ as shown in Fig. 4, the robot can generate the desired motion, though the burden of the human increases for generating the assistive force $^{ob}\boldsymbol{F}_{a_k}$. Under the relationship expressed by eq.(10), the feasible brake force $^{ob}\boldsymbol{F}_{w_k}$ should be derived within the feasible brake force set $A(U_j)$ so that the magnitude of the assistive force $^{ob}\boldsymbol{F}_{a_k}$ is as small as possible to reduce the burden of the human. This control method means that the robot can generate the virtual force in the region as shown in Fig. 5 by combining with the assistive force applied by the human $^{ob}\boldsymbol{F}_{a_k}$.

III. Object Handling by Multiple Passive Mobile Robots along Path

In this section, we consider a collaboration method of multiple passive mobile robots and explain the problem of the control constraint of the brake system for realizing

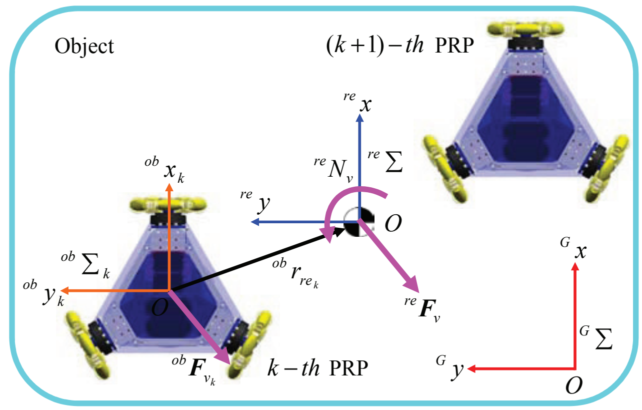

Fig. 6. Relationship between PRP and Representative Point of an Object

some functions. As an example of the functions realized by multiple robots, we pay attention to the object handling along the desired path. For realizing the path following function, we specify the virtual force and moment to the object based on the distance between the representative point of the object supported by the robots and the desired point along the path.

Firstly, we derive an apparent dynamics of an object around its representative point. Here, we define the object coordinate system $^{ob}\Sigma_k$ of k-th robot which is attached to on free joint of the k-th robot and the relative orientation between the $^{ob}\Sigma_k$ and $^{re}\Sigma$ is kept constant. $^{re}\Sigma$ is the coordinate system attached to the representative point of the object as shown in Fig. 6.

Based on the apparent dynamics of k-th PRP expressed in eq.(9), we can derive the dynamics of the object around its representative point, when the inertia and damping parameters satisfy the following equations.

$$\sum_{k=1}^{n} {}^{ob}\boldsymbol{M}_k \mathbf{P}_k^T = 0, \quad \sum_{k=1}^{n} {}^{ob}\boldsymbol{D}_k \mathbf{P}_k^T = 0 \tag{11}$$

where, $\mathbf{P}_k = [r_{y_k} \quad r_{x_k}]$ is a matrix defined by the element of the position vector $^{ob}\mathbf{r}_{re_k} = [r_{x_k} \quad r_{y_k}]^T$ from robot to the representative point of the object. This equation means that the representative point of the object is specified to the center of gravity position of the object. The apparent dynamics of the object around the representative point is expressed as follows:

$$\begin{aligned}&\begin{bmatrix} \sum {}^{ob}\boldsymbol{M}_k & \mathbf{0} \\ \mathbf{0} & \sum \mathbf{P}'_k {}^{ob}\boldsymbol{M}_k \mathbf{P}'^T_k \end{bmatrix} \begin{bmatrix} {}^{re}\ddot{\boldsymbol{q}}_{ob} \\ {}^{re}\ddot{\theta}_{ob} \end{bmatrix} \\ &+ \begin{bmatrix} \sum {}^{ob}\boldsymbol{D}_k & \mathbf{0} \\ \mathbf{0} & \sum \mathbf{P}'_k {}^{ob}\boldsymbol{D}_k \mathbf{P}'^T_k \end{bmatrix} \begin{bmatrix} {}^{re}\dot{\boldsymbol{q}}_{ob} \\ {}^{re}\dot{\theta}_{ob} \end{bmatrix} \\ &= \begin{bmatrix} {}^{re}\boldsymbol{F}_t + {}^{re}\boldsymbol{F}_v \\ {}^{re}N_t + {}^{re}N_v \end{bmatrix}\end{aligned} \tag{12}$$

where $\mathbf{P}'_k = [-r_{y_k} \quad r_{x_k}]$ and $^{re}\dot{\boldsymbol{q}}_{ob} \in \boldsymbol{R}^{2\times 1}$, $^{re}\ddot{\boldsymbol{q}}_{ob} \in \boldsymbol{R}^{2\times 1}$ are the velocity and the acceleration of the object around the representative point. $^{re}\boldsymbol{F}_t \in \boldsymbol{R}^{2\times 1}$ and $^{re}N_t \in R$ are the driving force and moment applied to the object by a human. $^{re}\boldsymbol{F}_v \in \boldsymbol{R}^{2\times 1}$ and $^{re}N_v \in R$ are virtual force and moment

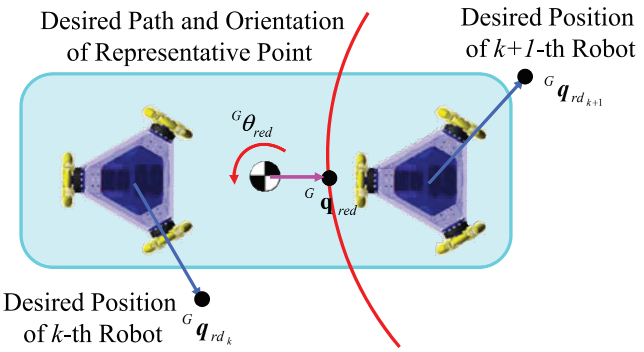

Fig. 7. Control for Path Following Based on Virtual Force/Moment

generated by each robot and are expressed as follows:

$$ {}^{re}\boldsymbol{F}_t = \sum_{k=1}^{n} {}^{ob}\boldsymbol{F}_{t_k}, \quad {}^{re}N_t = \sum_{k=1}^{n} (-{}^{ob}\mathbf{r}_{re_k} \times {}^{ob}\boldsymbol{F}_{t_k}) \quad (13) $$

$$ {}^{re}\boldsymbol{F}_v = \sum_{k=1}^{n} {}^{ob}\boldsymbol{F}_{v_k}, \quad {}^{re}N_v = \sum_{k=1}^{n} (-{}^{ob}\mathbf{r}_{re_k} \times {}^{ob}\boldsymbol{F}_{v_k}) \quad (14) $$

From eq.(12), we can control the position and orientation of the object based on the virtual force and moment.

For following along the desired path, our strategy is to compute the desired position of each PRP from the desired position/orientation of the object, and control each robot to converge on its desired position based on the virtual force as shown in Fig. 7. We can derive the desired position of each robot ${}^{G}\boldsymbol{q}_{rd_k} \in \boldsymbol{R}^{2\times1}$ with respect to the global coordinate system.

For moving k-th robot to its desired position, we design a general control method as follows:

$$ {}^{G}\boldsymbol{F}_{v_k} = \boldsymbol{K}_p({}^{G}\boldsymbol{q}_{rd_k} - {}^{G}\boldsymbol{q}_{r_k}) + \boldsymbol{K}_d({}^{G}\dot{\boldsymbol{q}}_{rd_k} - {}^{G}\dot{\boldsymbol{q}}_{r_k}) \quad (15) $$

where ${}^{G}\boldsymbol{q}_{r_k} \in \boldsymbol{R}^{2\times1}$ is the position of k-th robot. $\boldsymbol{K}_p \in \boldsymbol{R}^{2\times2}$, $\boldsymbol{K}_d \in \boldsymbol{R}^{2\times2}$ are constant matrices, respectively. By transforming the virtual force of eq.(15) to the ${}^{ob}\Sigma_k$ as ${}^{ob}\boldsymbol{F}_{v_k}$, the virtual force and moment are applied to the representative point of the object as shown in eq.(14), and the multiple robots control the position and orientation of the object.

It should be noted that passive robot cannot generate a virtual force to accelerate the robot as shown in Fig.5, because of the characteristics of the brake system depended on the rotational direction of each wheel. From this reason, if the virtual force has to generate along the acceleration direction of the robot, multiple robots could not control the position and orientation of the object precisely. For example, in the case of Fig. 8, the robots want to control the orientation of the object. But k-th PRP cannot generate the virtual force because the direction of the virtual force is the motion direction of the robot. In this case, the performance of the orientation control function would be decreased. In the next section, we discuss how to solve this problem and propose a method to improve the accuracy of the path following function with orientation control.

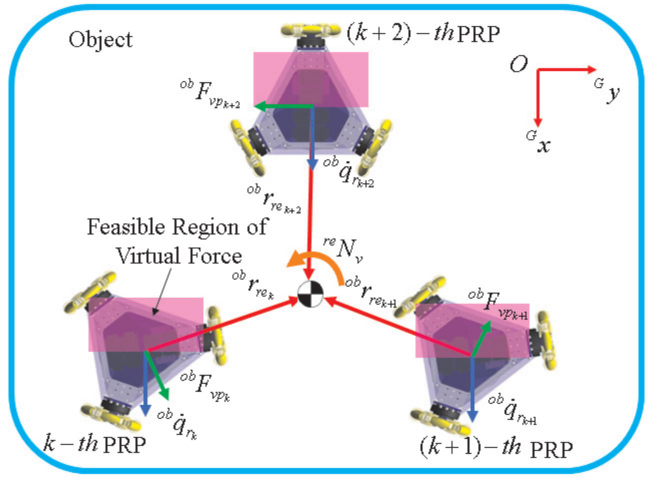

Fig. 8. Virtual Force for Controlling Orientation of an Object

IV. Distributed Control to Improve Path Following Performance

In this section, we especially consider a distributed motion control algorithm to generate the moment around the representative point of the object for controlling the orientation precisely. Each robot estimates whether all of the robots can generate the required virtual force or not. If some robots cannot generate the virtual force to control the orientation because of the feasible brake region as shown in Fig. 8, the other robots generate the force additionally to compensate the required virtual force/moment around the representative point of the object for controlling the orientation precisely.

Note that each robot does not need to communicate with other robots under the assumption that each robot knows the positions between all robots and the representative point of an object in advance, because each robot can calculate the virtual force of all robots by using the desired position and orientation of the representative point of the object and the positions of the other robots.

Firstly, k-th robot computes its own position and the positions of the other robots ${}^{G}\boldsymbol{q}_{r_i} \in \boldsymbol{R}^{2\times1}$ based on the relationship between the positions of the representative point of the object and i-th robot. Note that subscript i represents the robot from 1-th to n-th including k-th. Thus, $i = 1, 2, \cdots, k \cdots, n$. k-th robot also calculates the desired position of the other robots ${}^{G}\boldsymbol{q}_{rd_i} \in \boldsymbol{R}^{2\times1}$ from the desired orientation of the object ${}^{G}\theta_{red} \in R$. From the position and velocity of i-th robot, k-th robot can calculate the virtual force of i-th robot ${}^{G}\boldsymbol{F}_{v_i} \in \boldsymbol{R}^{2\times1}$ as same as eq.(15).

$$ {}^{G}\boldsymbol{F}_{v_i} = \boldsymbol{K}_p({}^{G}\boldsymbol{q}_{rd_i} - {}^{G}\boldsymbol{q}_{r_i}) + \boldsymbol{K}_d({}^{G}\dot{\boldsymbol{q}}_{rd_i} - {}^{G}\dot{\boldsymbol{q}}_{r_i}) \quad (16) $$

where $\boldsymbol{K}_p \in \boldsymbol{R}^{2\times2}$, $\boldsymbol{K}_d \in \boldsymbol{R}^{2\times2}$ are constant matrices, respectively.

Next, we consider how to estimate whether each robot can generate the virtual force ${}^{G}\boldsymbol{F}_{v_i}$ or not. For the simplicity of the following discussion, we transform the velocity of each robot ${}^{G}\dot{\boldsymbol{q}}_{r_i}$ and the virtual force ${}^{G}\boldsymbol{F}_{v_i}$ to the object coordinate system of each robot as follows:

$$ {}^{ob}\dot{\boldsymbol{q}}_{r_i} = {}^{G}\boldsymbol{R}_{ob}^{-1}{}^{G}\dot{\boldsymbol{q}}_{r_i} \quad , \quad {}^{ob}\boldsymbol{F}_{v_i} = {}^{G}\boldsymbol{R}_{ob}^{-1}{}^{G}\boldsymbol{F}_{v_i} \tag{17} $$

where, ${}^{G}\boldsymbol{R}_{ob} \in \boldsymbol{R}^{2\times 2}$ is the rotation matrix represented by the orientation of the object ${}^{G}\theta_{ob}$. Passive mobile robot cannot generate the virtual force along the moving direction of the robot as shown in Fig. 5, that is, i-th robot cannot generate the virtual force ${}^{ob}\boldsymbol{F}_{v_i}$ when the angle $\theta_i \in R$ between the velocity direction of each robot ${}^{ob}\dot{\boldsymbol{q}}_{r_i}$ and the direction of the virtual force ${}^{ob}\boldsymbol{F}_{v_i}$ satisfies the following inequality.

$$ \theta_i < 90^\circ \tag{18} $$

The angle θ_i is derived as follows:

$$ \theta_i = \cos^{-1}\left(\frac{{}^{ob}\dot{\boldsymbol{q}}_{r_i} \cdot {}^{ob}\boldsymbol{F}_{v_i}}{\left|{}^{ob}\dot{\boldsymbol{q}}_{r_i}\right| \left|{}^{ob}\boldsymbol{F}_{v_i}\right|}\right) \tag{19} $$

From eq.(18) and eq.(19), the virtual force ${}^{ob}\boldsymbol{F}_{v_i}^{un}$ that i-th robot cannot generate it is expressed as follows:

$$ {}^{ob}\boldsymbol{F}_{v_i}^{un} = \begin{cases} {}^{ob}\boldsymbol{F}_{v_i} & \text{if } (\theta_i < 90^\circ) \\ \boldsymbol{0} & \text{otherwise} \end{cases} \tag{20} $$

The short of the virtual moment ${}^{re}N_v^{un} \in R$ around the representative point of the object is derived as eq.(21).

$$ {}^{re}N_v^{un} = \sum_{i=1}^{n} \left(-{}^{ob}\mathbf{r}_{re_i} \times {}^{ob}\boldsymbol{F}_{v_i}^{un}\right) \tag{21} $$

For compensating the insufficient virtual moment, robots that can generate the virtual force generate the additional virtual force. There are many solutions for deriving the virtual force of each robot to compensate the insufficient virtual moment shown in eq.(21). In this research, we distribute the short of the virtual force equally to each robot that can generate the virtual force as follows:

$$ \left|{}^{ob}\boldsymbol{F}_v^{*}\right| = \frac{\left|{}^{re}N_v^{un}\right|}{\sum_{i=1}^{n} \left|{}^{ob}\acute{\mathbf{r}}_{re_i}\right|} \tag{22} $$

where $\left|{}^{ob}\boldsymbol{F}_v^{*}\right|$ is the absolute value of the insufficient virtual force which is equerry distributed to each robot that can generate the virtual force. $\left|{}^{ob}\acute{\mathbf{r}}_{re_i}\right|$ expresses the distance between each robot and the representative point of the object ${}^{ob}\mathbf{r}_{re_i} = [r_{x_i} \quad r_{y_i}]^T$ as follows:

$$ \left|{}^{ob}\acute{\mathbf{r}}_{re_i}\right| = \begin{cases} 0 & \text{if } (\theta_i < 90^\circ) \\ \left|{}^{ob}\mathbf{r}_{re_i}\right| & \text{otherwise} \end{cases} \tag{23} $$

${}^{ob}\boldsymbol{F}_v^{*}$ are also expressed as following equation with respect to x and y components of the virtual force of k-th robot.

(i) for $\theta_k < 90^\circ$

$$ {}^{ob}f_{vx_k}^{*} = 0 \tag{24} $$

$$ {}^{ob}f_{vy_k}^{*} = 0 \tag{25} $$

(ii) for $\theta_k \geq 90^\circ$

$$ {}^{ob}f_{vx_k}^{*} = |{}^{ob}\boldsymbol{F}_v^{*}| \cos\left(|{}^{ob}\theta_{re_k}|\right) \operatorname{sgn}({}^{ob}f_{vx_k}) \tag{26} $$

$$ {}^{ob}f_{vy_k}^{*} = |{}^{ob}\boldsymbol{F}_v^{*}| \sin\left(|{}^{ob}\theta_{re_k}|\right) \operatorname{sgn}({}^{ob}f_{vy_k}) \tag{27} $$

where ${}^{ob}\theta_{re_k}$ is the angle based on the positional relationship between each robot and the representative point of the object ${}^{ob}\mathbf{r}_{re_k} = [r_{x_k} \quad r_{y_k}]^T$ as follows:

$$ {}^{ob}\theta_{re_k} = \tan^{-1}\left(\frac{r_{x_k}}{r_{y_k}}\right) \tag{28} $$

We transform the virtual force ${}^{ob}\boldsymbol{F}_v^{*}$ derived by eq.(24), eq.(25), eq.(26) and eq.(27) to the global coordinate system ${}^{G}\Sigma$ by the rotation matrix ${}^{G}\boldsymbol{R}_{ob}$ as follows:

$$ {}^{G}\boldsymbol{F}_{v_k}^{*} = {}^{G}\boldsymbol{R}_{ob}{}^{ob}\boldsymbol{F}_{v_k}^{*} \tag{29} $$

Finally, the virtual force ${}^{G}\boldsymbol{F}_{v_k}$ of k-th robot is generated based on the following equation by rewriting eq.(15).

$$ {}^{G}\boldsymbol{F}_{v_k} = \boldsymbol{K}_p({}^{G}\boldsymbol{q}_{rd_k} - {}^{G}\boldsymbol{q}_{r_k}) + \boldsymbol{K}_d({}^{G}\dot{\boldsymbol{q}}_{rd_k} - {}^{G}\dot{\boldsymbol{q}}_{r_k}) + {}^{G}\boldsymbol{F}_{v_k}^{*} \tag{30} $$

By using above method, we can compensate the insufficient virtual moment that is needed to control the orientation of the handling object precisely.

V. Experiments for Handling an Object

We experimented with two PRPs for handling a single object to illustrate the validity of the proposed control algorithm. In the experiments, we utilized the motion control algorithm explained in section III, which did not distribute the insufficient virtual force among robots, and the proposed distributed motion control algorithm explained in section IV. In both of them, we set the desired path at the representative point of the object as shown in Fig. 9 and the desired orientation is the tangential direction of the desired path, and them the path following control was realized based on the virtual force/moment generated by the brake system.

Experimental results are illustrated in Fig. 10 - Fig. 12. In Fig. 10 expresses the path of each PRP, the path of the representative point of the object, and the comparison between the non-distributed algorithm and the proposed distributed

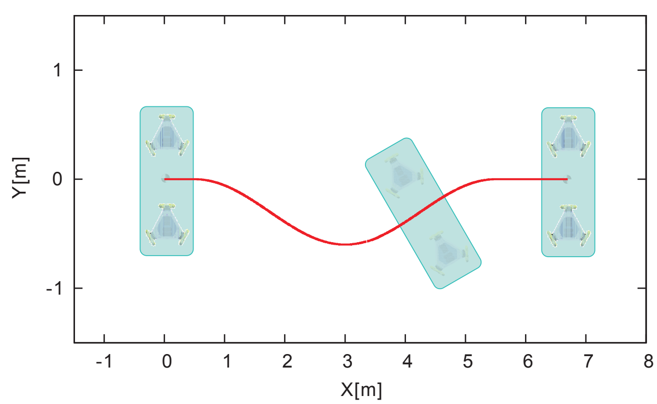

Fig. 9. Desired Path of Representative Point of an Object

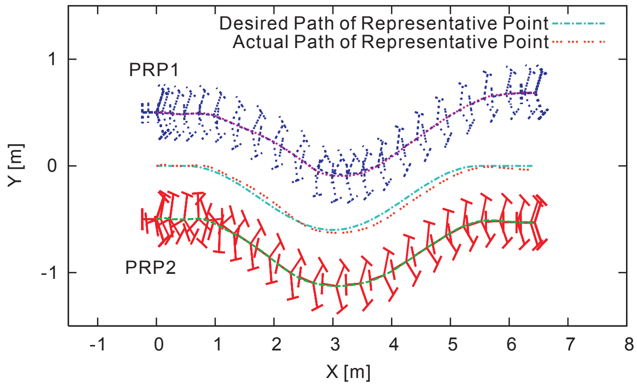

(a) Non-distributed Algorithm

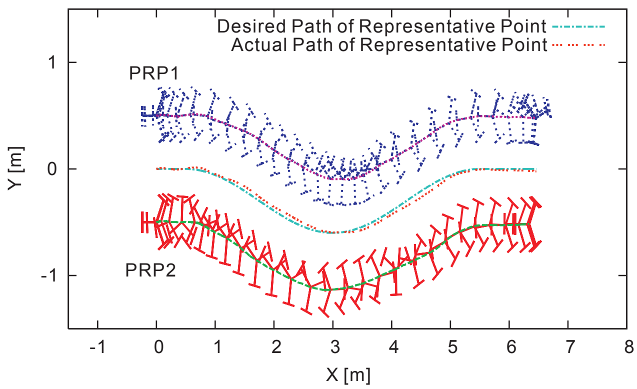

(b) Distributed Algorithm

Fig. 10. Experimental Results of Path Following

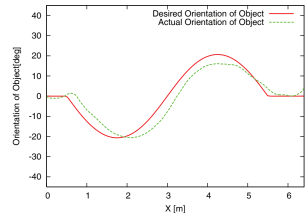

(a) Non-distributed Algorithm

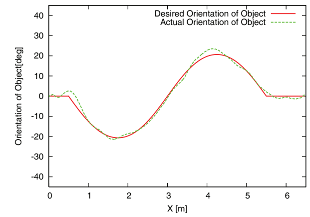

(b) Distributed Algorithm

Fig. 11. Experimental Results of Orientation Control

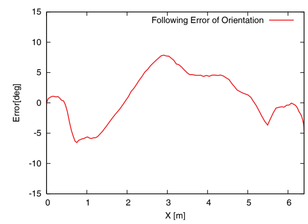

(a) Non-distributed Algorithm

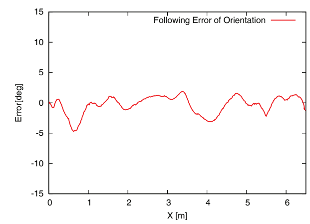

(b) Distributed Algorithm

Fig. 12. Error of Orientation Control

algorithm. Regarding to the position error, we cannot see large errors in both the non-distributed algorithm and the proposed distributed algorithm. Fig. 11 is the orientation of the handling object with respect to time. We also show the following error of the orientation in Fig. 12. From these figures, we can see that the following error of the orientation by the proposed algorithm is smaller compared to the following error by the non-distributed algorithm. From these experimental results, we illustrated that the multiple passive robots distributed the required virtual force appropriately and the performance of the object handling was improved.

VI. Conclusions

This paper considered the control problem of the passive mobile robot with servo brakes. Servo brake cannot generate the force for accelerating the system, so that the performance of the functions realized by passive robots might be decrease. In this paper, we paid attention to the collaboration of multiple passive mobile robots for handling a large object, and proposed the distributed motion control algorithms for them, in which each robot compensated the required control input of other robots which cannot generate it because of the brake constraint. The proposed algorithm applied to two passive mobile robots called PRP experimentally and realized the object handling along the desired path for illustrating the validity of the proposed algorithm. The proposed control algorithm could be applied to not only path following control but also the other functions such as collision avoidance, when some robots cannot generate the sufficient virtual force for controlling them.

As the future works, we should consider the maximum feasible force of each robot. In some situations, the robots could not distribute the required force/moment equally among robots that can generate the braking force, because of the braking torque limitation of each robot. Based on the tasks and the braking torque limitation of each wheel of the robots, we should adjust the ratio of the distributed force among robots.

References

[1] A. Goswami, M. A. Peshkin, J. Colgate,"Passive robotics: an exploration of mechanical computation",*Proc. of the IEEE Int. Conf. on Robotics and Automation*, pp.279-284, 1990.

[2] M. A. Peshkin, J. E. Colgate, W. Wannasuphoprasit, C. A. Moore, R. B. Gillespie, P.Akella, "Cobot Architecture", *IEEE Transactions on Robotics and Automation*, Vol. 17, No.4, 2001.

[3] Y. Hirata, A. Hara, K.Kosuge,"Passive-type Intelligent Walking Support System -RT Walker-", *Proceedings of the 2004 IEEE/RSJ Int. Conf. on Intelligent Robots and Systems*, pp.2289-2294, 2004.

[4] K. Fukaya, Y. Hirata, Z. D. Wang, K. Kosuge, "Design and Control of A Passive Mobile Robot System for Object Transportation", *Proc. of IEEE Int. Conf. on Mechtronics and Automation*, pp.31-36, 2006.

[5] Y. Hirata, K. Kosuge, "Distributed Robot Helpers Handling a Single Object in Cooperation with a Human", *Proc. of IEEE Int. Conf. on Robotics and Automation*, pp.458–463, 2000.

[6] O. Khatib, K. Yokoi, K. Chang, D. Ruspini, R. Holmberg, and A. Casal, "Coordination and Decentralized Cooperation of Multiple Mobile Manipulators", *Journal of Robotic Systems*, pp.755-764, 1996.

[7] Y. Hirata, T. Takagi, K. Kosuge, H. Asama, H. Kaetsu, K. Kawabata, " Manipulation of a Large Object by Multiple DR Helpers in Cooperation with a Human", *Proc. of IEEE International Conference on Intelligent Robots and Systems*, pp.126-131, 2001.

[8] Y.Hirata, H. Song, Z. Wang, K. Kosgue, "Control of Passive Object Handling Robot with Free Joint for Reducing Human Assistive Force", *Proc. of IEEE Int. Conf. on Intelligent Robots and Systems*, pp.1154-1159, 2007.